J. Fluid Mech. (1981), *vol.* 109, *pp.* 75–87
Printed in Great Britain

Thermal convection in a rotating fluid: effects due to bottom topography

By HARRY LEACH†
Geophysical Fluid Dynamics Laboratory, Meteorological Office, Bracknell, England

(Received 26 January 1980 and in revised form 10 November 1980)

A study has been made of the effects of non-axisymmetric bottom topography in a differentially heated, rotating fluid annulus. In the absence of free baroclinic waves the disturbance produced by topography of vertical dimensions typically much less than the depth of the fluid and horizontal dimensions comparable to the gap width is steady and confined to the lower part of the fluid. The maximum amplitude of this disturbance depends on the angular speed of rotation of the apparatus and varies with height, being very small above the level where the basic azimuthal flow reverses. The flow pattern shows a closed circulation displaced relative to the topography in the downstream direction. In the presence of free baroclinic waves the topographic wave extends throughout the whole depth of the fluid. Determinations of the amplitude and phase of the various azimuthal Fourier components present show that the topographically forced components exchange energy with the free components as they drift relative to the topography.

1. Introduction

The effect of bottom topography on the dynamics of rotating, thermally convecting fluids is of great interest for a number of geophysical systems. The present work concerns laboratory experiments conducted to investigate some of these effects. The apparatus used was an annulus; an annular tank of fluid whose inner and outer walls are maintained at different temperatures and which rotates uniformly and steadily about its vertically-arranged axis of symmetry. The experiments show that bottom topography can produce disturbances in a system that would otherwise have axisymmetric flow and that when free waves are also present these disturbances undergo nonlinear interactions with the topographically generated waves.

Previous experiments in which purely axisymmetric boundaries were used (see Hide & Mason 1975 for a review) show the existence of a variety of flow regimes depending on the applied conditions of temperature difference and rotation speed. The flow regimes can be basically divided into two classes; namely those in which the flow is characterized by axial symmetry and those where the flow is non-axisymmetric. In this work the term symmetric will be used to describe flows which would be axisymmetric in the absence of topography. The regular or irregular waves that are seen in non-axisymmetric flows are produced by a mechanism known as baroclinic instability. This instability was investigated theoretically by Eady (1949). For quasi-geostrophic

† Present address: Institut für Meereskunde, Düsternbrooker Weg 20, D-2300 Kiel 1, FRG.

flows with large Richardson number the presence or absence of growing perturbations was found to depend on the parameter

$$B = -\frac{g(\partial\rho_0/\partial z)d^2}{4\Omega^2\bar{\rho}(b-a)^2},$$

where g is the acceleration due to gravity, $\partial\rho_0/\partial z$ is the basic vertical density gradient, d the depth of the fluid, Ω the apparatus rotation speed, $\bar{\rho}$ the mean density of the fluid and a and b the inner and outer radii of the annulus. If $B > 0{\cdot}583$ all modes would be stable but if $B < 0{\cdot}583$ long waves would grow. These results were found to be in reasonable agreement with experiments.

Studies of rotating stratified flow over topography have now been reported by a number of authors. An experimental investigation of Taylor columns in a stratified flow was made by Davies (1972) who showed that the disturbance due to his spherical obstacle extended to many times the height of the obstacle when $Nf^{-1} \lesssim 0{\cdot}1$. Theoretical studies of this problem have been made by Hogg (1973), Huppert (1975) and Redekopp (1975). Earlier studies of the homogeneous case ($B = 0$) by Hide (1961), Hide & Ibbetson (1966) and Ingersoll (1969) had identified

$$S = h/dR,$$

where h is the height of the topography, d the fluid depth and R a Rossby number based on the horizontal length scale of the topography, as the crucial parameter in the Taylor-column problem; when $S \gtrsim 2$ a Taylor column can form. Hogg (1973) showed that in the stratified case ($B > 0$) S takes a critical value larger than 2 when $B > 1$ and when $B \gg 1$, the critical value of S tends to B. Huppert (1975) subsequently showed that in the stratified case closed circulations could occur for obstacles with any S if they had vertical sides. In the present study little difference was observed between obstacles with vertical sides and smooth obstacles but this may be attributed to the experimental flow not being quasi-geostrophic and being slightly viscous.

These authors all avoided the problem of sheared flows with a level-of-no-motion, a reversal at some level within the flow. As discussed by de Szoeke (1972) this leads to the possibility of topographically forced baroclinic waves. The results presented below also show that the presence of a flow reversal leads to effects not considered in the stratified Taylor column studies. Fultz & Spence (1967) reported observing lee waves downstream of a ridge placed in an annulus.

In a paper on spatially growing baroclinic waves Hogg (1976) has shown that it is possible for the equations for a simple baroclinic flow to have spatially growing solutions with vertical structures similar to those reported below. It is, however, unfortunately not easily possible to compare his results quantitatively with those presented here.

Visual observations of the effects of topography on free baroclinic waves in the annulus have been reported by Kester (1966), Fultz & Spence (1967) and Yeh & Chang (1974). In all these papers the authors describe how the wave lobes are distorted in the region of the topography. In this paper I present the results of experiments in which these interactions are analysed in terms of single Fourier components.

In a recent paper on baroclinic flow over topography Charney & Straus (1980) have

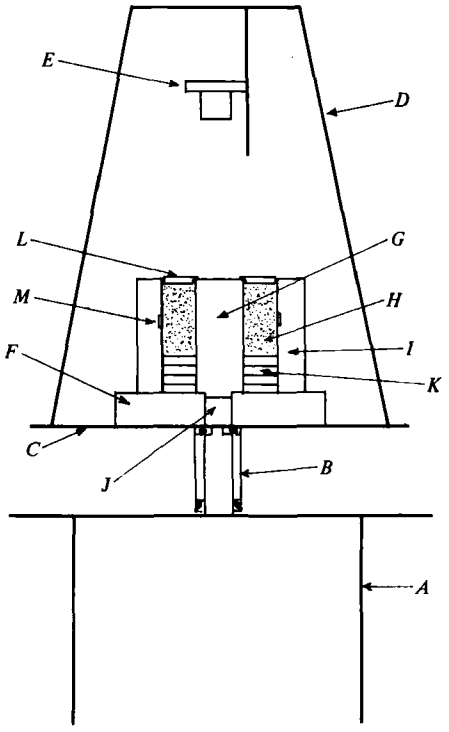

FIGURE 1. Detailed diagram of experimental apparatus showing annulus mounted on turntable. The drive system is not shown. *A*, stand; *B*, bearing assembly; *C*, turntable; *D*, tripod; *E*, camera; *F*, base; *G*, inner bath; *H*, working fluid; *I*, outer bath; *J*, fluid slip ring; *K*, false bases; *L*, lid; *M*, window.

made use of a two-layer, quasi-geostrophic spectral, numerical model. They show that topography can produce disturbances in a flow that would be otherwise stable and that spontaneous baroclinic instability is modified by the presence of topography.

2. Apparatus & Procedure

The apparatus (see figure 1) was similar to that used in other annulus experiments (for example see Douglas, Hide & Mason 1972). The thermocouple arrays used to measure temperatures in the fluid were suspended from the lid. The topography was made either from pieces of acrylic cut to the desired form or by laminating thin sheets of light alloy. Observation of flow patterns was made by streak photography (see Douglas *et al.* 1972). The principal working fluid was a 15% solution of glycerol in water of viscosity 1·32 $mm^2\ s^{-1}$ and density 1·028 $Mg\ m^{-3}$ containing 0·5 mm diameter polystyrene beads which are neutrally buoyant in this solution. In all experiments a wall-to-wall temperature difference of 10 K was used.

In the rotating lid experiment five thermocouples were used arranged vertically in a row on a single constantan wire suspended from the lid. A diagram of the rotating lid appears in figure 2. The thermocouple array was moved very slowly through the fluid over the topography to investigate the disturbance due to the topography at different

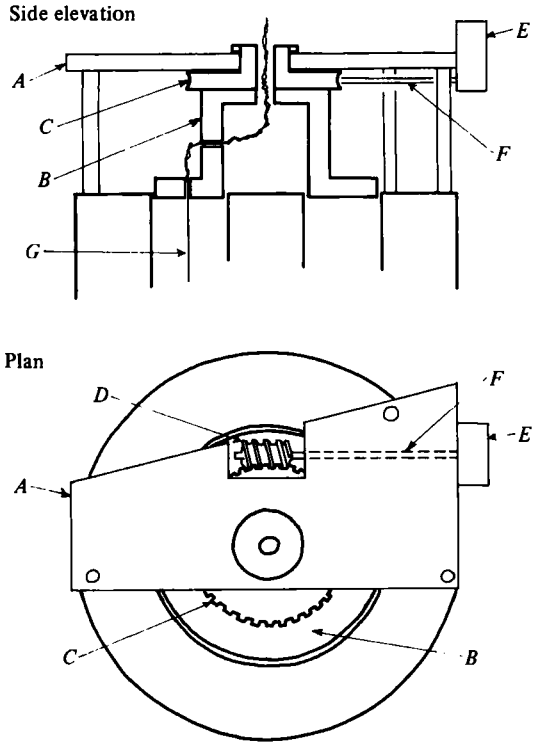

FIGURE 2. Diagram of rotating lid used to move thermocouple array for measuring stationary, topographic waves. The lid itself is 'top-hat'-shaped and suspended from the support so that it is just in contact with the working fluid. Drive is by a small electric motor through a worm and wheel. *A*, tripod support standing on top of annulus; *B*, rotating lid; *C*, gear wheel; *D*, worm gear; *E*, electric motor; *F*, drive shaft; *G*, thermocouple probe.

levels and azimuths in the flow. In the spectral analysis experiments a ring of constantan wire was positioned around the annulus in the centre of the channel and sixteen individual copper wires soldered to it at regular azimuthal spacing. The voltages from the thermocouples were measured and recorded automatically on computer-compatible media by an electronic data-acquisition system. In the rotating lid experiment the temperatures at each of the five different levels were sampled every 4 s so that a series of 450 points for each level was obtained during a single revolution of the lid, which took 30 minutes. These series were subjected to Fourier decomposition so that the amplitude of each stationary wave number could be found at the five levels. From the difference of the mean temperatures at the highest and lowest levels a mean vertical temperature gradient $(\partial T_0/\partial z)$ was found which could be used to calculate the parameter B. In the spectral analysis experiments the temperatures at the sixteen points around the ring were sampled sufficiently frequently to avoid aliasing high frequency signals and for sufficiently long to allow several wave lobes to pass a given point within the annulus. Each scan of the temperatures was Fourier analysed in order to observe how the energy was distributed between the different spectral components and how this distribution varied in time.

3. Experimental results

Symmetric regime

Observations of the flow patterns associated with isolated bottom topography in the symmetric regime were made using streak photography. Near the mid-level of the fluid, where the zonal motion due to the thermal wind effect is relatively small, conditions for the observation of disturbances in the flow are best. At low rotation speeds little disturbance was visible, figure 3(*a*), but at higher rotation speeds, lower B, figure 3(*b*), a distinct closed circulation could be seen. This feature lies to the west of the topography, which is the downstream side for flow in the lower part of the annulus. For similar experimental conditions and topographic heights the shape of the topography did not noticeably affect the form of the disturbance; even the smooth topography with zonal wavenumber 3 had a closed circulation associated with each peak. Huppert's (1975) results expect a dependence on the shape of the topography but his theory was for an inviscid and quasi-geostrophic flow, which is not the case in these experiments.

In order to investigate the nature of the disturbance more closely measurements were made of the temperature at five different levels in the flow by means of a rotating lid which carried an array of thermocouples. In these experiments topography of the form

$$h = h_0 \sin m\phi \sin \pi \frac{(r-a)}{(b-a)}, \quad a < r < b$$

was used. Here r and ϕ are the radial and azimuthal co-ordinates, m the azimuthal wavenumber of the topography and a and b the inner and outer radii of the annulus. The temperatures measured as a function of azimuth at the five levels were subject to Fourier decomposition. The principle result of this analysis is that the disturbance of the temperature field as represented by the amplitude of the forced wavenumber is confined to the lower half of the fluid below the level of no motion, see figure 4. This shows the amplitude of the disturbance as a function of depth for a series of different values of B. The amplitude is normalized by the product of the topographic height and the mean vertical temperature gradient $(h_0(\partial T_0/\partial z))$. The size of the error bars were determined by conducting control experiments without topography and processing the data obtained in the same way as for experiments with topography, the amplitudes obtained without topography were taken to be the error in the measurements with topography. The lines joining the data points are not supposed to represent any functional form but serve merely to connect points measured for a particular value of B. As can be seen from figure 4 the amplitude of the disturbance increases with increasing apparatus rotation speed; the amplitude of the disturbance at the second level from the bottom as a function of $B^{\frac{1}{2}}$ is shown in figure 5. The straight line drawn through the points is a linear regression in the semi-logarithmic plane. The reason for trying this fit was the expectation from geostrophic theory (see Robinson 1960) that

$$\text{amplitude} \propto \exp(-B^{\frac{1}{2}} kz),$$

where k is the wavenumber of the topography and z the vertical co-ordinate. The assumption of geostrophy for these experiments is not good (the Rossby number is perhaps 0·1) but despite that the straight line fits the data reasonably well.

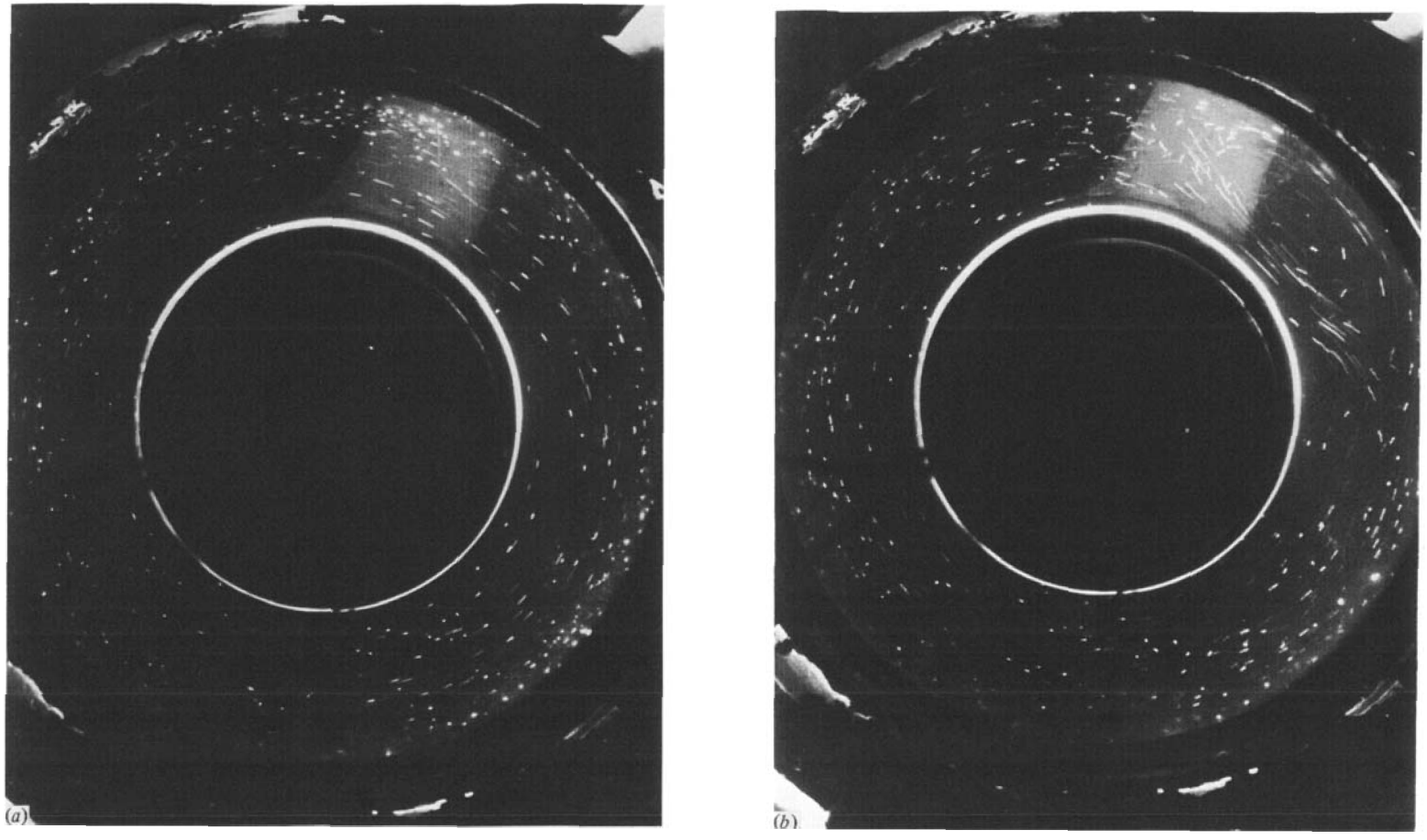

FIGURE 3. Streak photographs of flows above topography. The topography is a smooth isolated ridge situated at 'one o'clock'. Its height is 8% of the depth of the fluid ($h/d = 0{\cdot}08$) and the level of observation is at 39% of the tank depth from the bottom. The aspect ratio ($d/(b-a)$) of the annulus is 2·60. (*a*) shows only slightly deflected streamlines, $\Omega = 0{\cdot}25$ rad s^{-1}, $B = 5{\cdot}9$, $Nf^{-1} = 0{\cdot}93$. (*b*) shows closed circulation, $\Omega = 0{\cdot}51$ rad s^{-1}, $B = 1{\cdot}51$, $Nf^{-1} = 0{\cdot}47$.

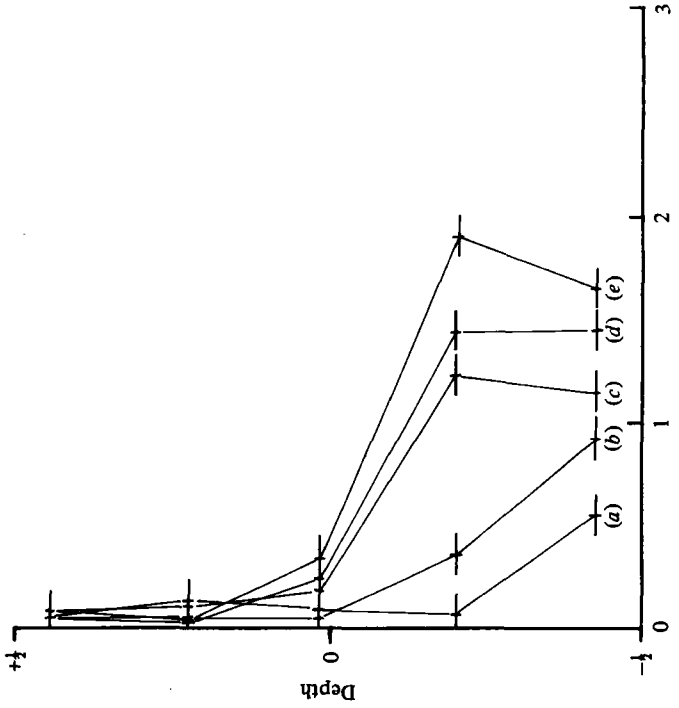

FIGURE 4. Graphs of dimensionless amplitude *vs.* dimensionless depth from rotating lid experiments showing the effect of varying the apparatus rotation speed, Ω. The amplitudes are those of wavenumber 3 which was the forcing wavenumber. $d/(b-a) = 3{\cdot}44$, $h_0/d = 0{\cdot}035$

	Ω(rad s^{-1})	Nf^{-1}	B
(*a*)	0·23	0·77	6·96
(*b*)	0·42	0·45	2·39
(*c*)	0·59	0·32	1·22
(*d*)	0·82	0·24	0·69
(*e*)	1·05	0·19	0·44

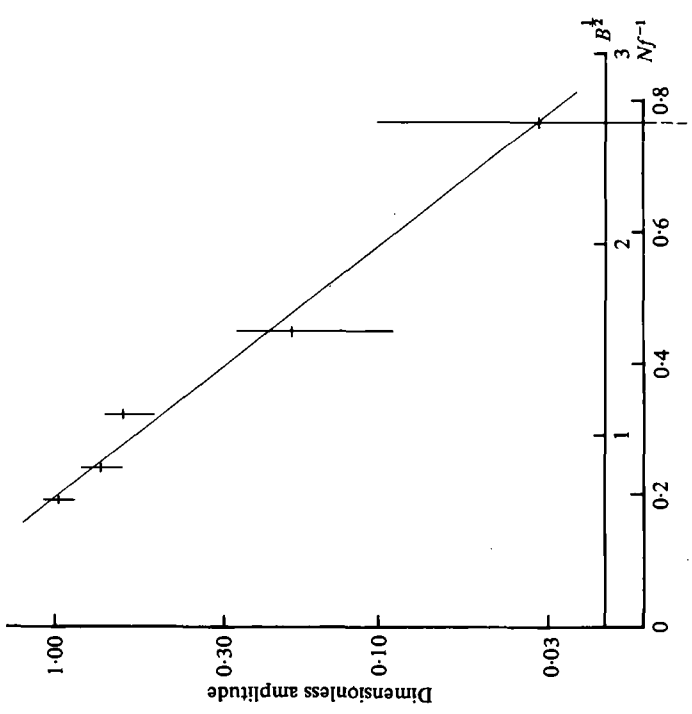

FIGURE 5. The variation of the logarithm of the amplitude of the topographic disturbance as a function of $B^{\frac{1}{3}}$ and Nf^{-1}. The amplitude is that at the second level from the bottom in figure 4 at a dimensionless height of 25% of the fluid depth from the bottom. $m = 3$, $d/(b-a) = 3{\cdot}44$ and $h_0/d = 0{\cdot}035$. The straight line is a linear regression in the semi-logarithmic plane.

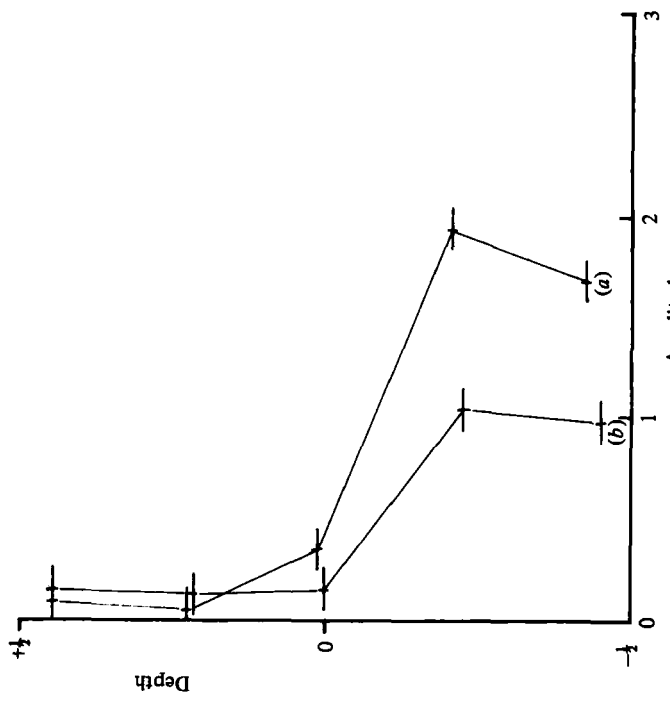

FIGURE 7. Graphs of dimensionless amplitude of the forced wavenumber *vs.* dimensionless depth from rotating lid experiments showing the effect of varying the wavenumber m of the topography. In both cases $\Omega = 1{\cdot}05$ rad s^{-1}, $Nf^{-1} = 0{\cdot}19$, $B = 0{\cdot}44$. (*a*) $m = 3$, $h_0/d = 0{\cdot}035$; (*b*) $m = 1$, $h_0/d = 0{\cdot}062$.

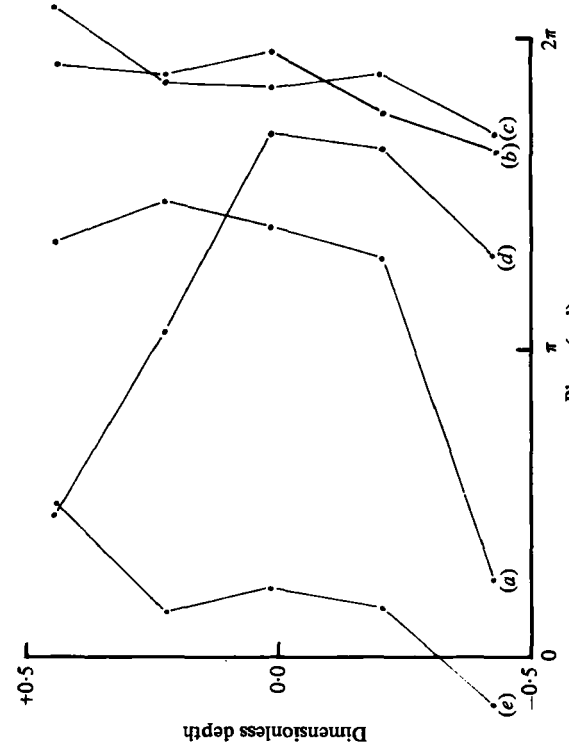

FIGURE 6. Graphs of phase against depth for the amplitude curves presented in figure 4. The absolute value of the phase is arbitrary.

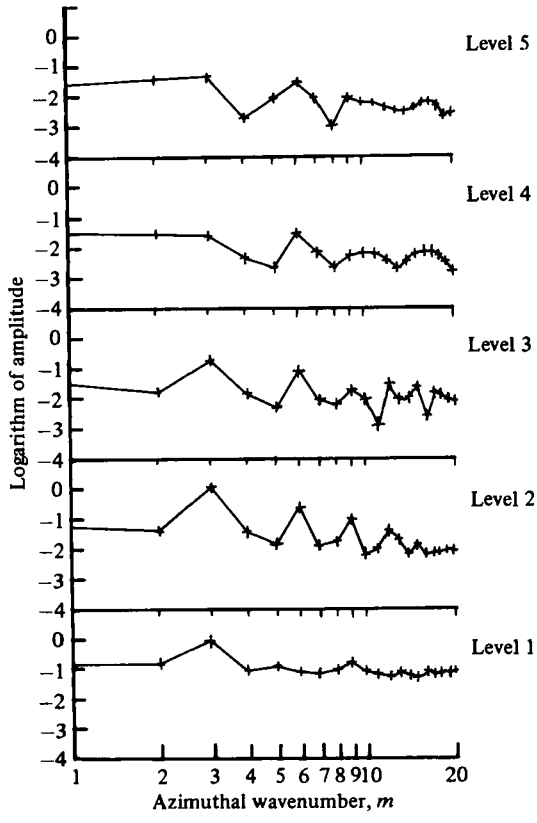

FIGURE 8. Spectra of the topographically forced disturbance at the five levels of observation for the case $\Omega = 1{\cdot}05$ rad s^{-1}, $Nf^{-1} = 0{\cdot}19$, $B = 0{\cdot}44$; $d/(b-a) = 3{\cdot}44$, $h_0/d = 0{\cdot}035$. Note the predominance of the forced wavenumber, $m = 3$, and its harmonics.

The dependence of the amplitude on z for a particular value of B is clearly less in agreement with the simple theory at lower values of B (figure 4).

The variation of phase with height for the runs shown in figure 4 is shown in figure 6. Some of the results show a steady rate of change of phase with height with a phase shift of about 1 radian between top and bottom. This is not always the case but for the profile in question, d, the amplitude at the highest levels is very small indeed and in principle indeterminate.

Robinson's (1960) theory predicts no change of phase with height. In the time-independent case the phase shift with height is due to Ekman pumping (Leach 1975); the time for a single fluid particle to pass over the topography is a few seconds compared with a spin-up time of about two minutes.

The amplitude at the forced wavenumber was also found to vary with the azimuthal wavenumber of the topography. Figure 7 shows curves for similar conditions for $m = 1$ and $m = 3$ which show that the maximum amplitude of the disturbance is larger for $m = 3$.

In figure 4 we saw the vertical structure of the disturbance at the forced wavenumber, $m = 3$. In figure 8 spectra of all the forced waves are shown and it can be seen that besides the forced wave number its harmonics also have relatively large amplitudes.

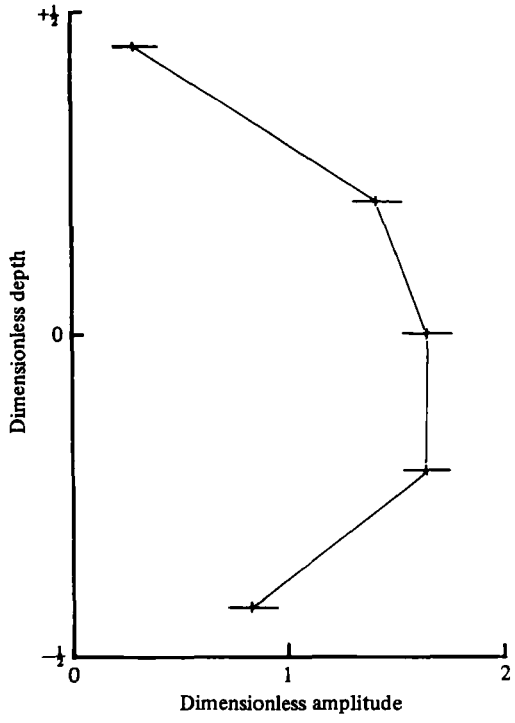

FIGURE 9. Dimensionless amplitude *vs.* dimensionless depth of topographically forced wave in the presence of spontaneous baroclinic waves showing that the topographic disturbance is not confined to the lower part of the fluid. $\Omega = 2{\cdot}94$ rad s^{-1}, $Nf^{-1} = 0{\cdot}082$, $B = 0{\cdot}037$, $d/(b-a) = 2{\cdot}34$, $m = 3$, $h_0/d = 0{\cdot}050$.

Wave regime

In the presence of spontaneous baroclinic waves the topographic disturbance fills the whole depth of the fluid, see figure 9. As in the symmetric regime the forced wave and its harmonics predominates, see figure 10.

Observations of the wave pattern were made using still and cine photography and these showed that in some cases the waves were severely disrupted by isolated topography. Near the mid-level, where the zonal motions are weak relative to the eddy motions, the passage of a wave over the ridge could be followed in detail. As a wave lobe approached from the west it slowed down and then broke up as it passed over the ridge and did not reform until about 90° to the east. This agrees with the observations of Kester (1966) and Fultz & Spence (1967). In order to observe these phenomena in terms of wave interactions, measurements of wave spectra were made using the thermocouple ring technique, see Hide, Mason & Plumb (1977) who used this technique to study the interactions of the spontaneous waves with each other. Spatial Fourier analyses of the temperatures measured around the ring were conducted and the variation in time of the amplitudes and phases of the different wave numbers observed. This revealed that at relatively low rotation speeds the dominant components of the topographic and drifting waves exchanged energy over a period equal to that required for the drifting wave pattern to move by one lobe. This is shown in figure 11 where the amplitude and phase of the dominant wave numbers are plotted against time and it can be seen that the amplitudes of the topographic and drifting waves are in antiphase.

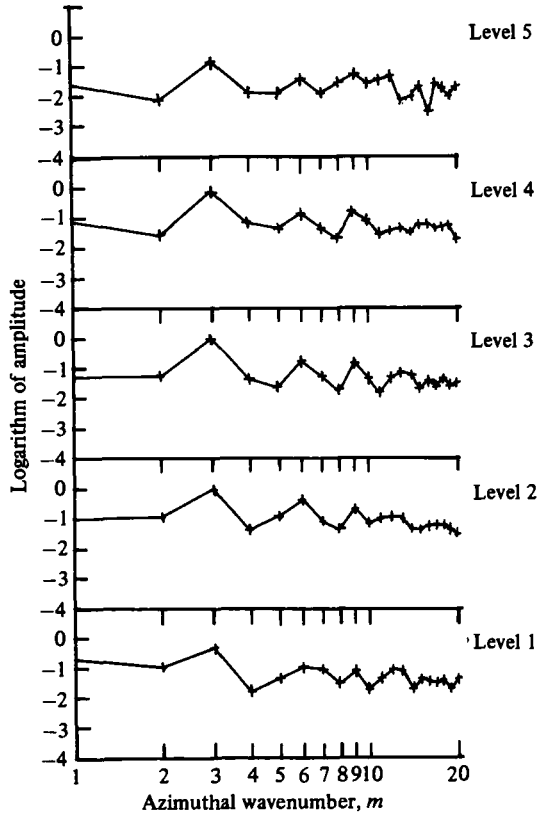

FIGURE 10. Spectra of the topographically forced disturbance at the five levels of observation in a flow containing spontaneous baroclinic waves. $\Omega = 2{\cdot}94$ rad s^{-1}, $Nf^{-1} = 0{\cdot}082$, $B = 0{\cdot}037$, $d/(b-a) = 2{\cdot}34$, $h_0/d = 0{\cdot}050$. Notice how the forced wave, $m = 3$, and its harmonics penetrate to the top of the flow.

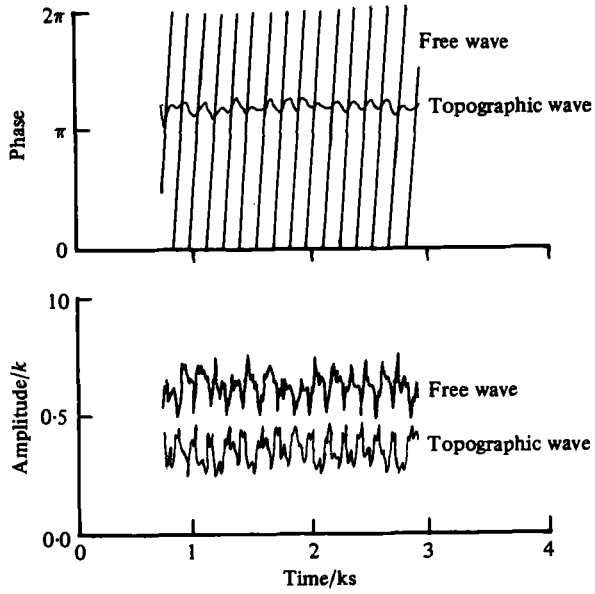

FIGURE 11. Amplitude and phase plotted against time for topographic and free waves. The topography was an isolated ridge with $h/d = 0{\cdot}083$; $d/(b-a) = 2{\cdot}60$, $\Omega = 2{\cdot}0$ rad s^{-1}. the wall-to-wall temperature difference was 11·9 K, $B \approx 0{\cdot}12$. The topographic wave was $m = 1$ and the free wave was $m = 3$. Note the antiphase relationship of their amplitudes.

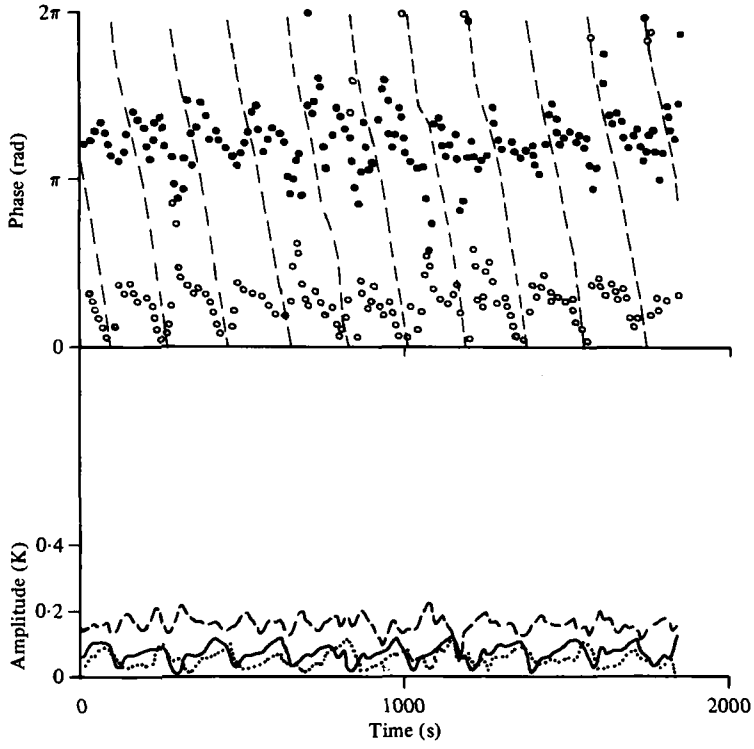

FIGURE 12. Amplitude and phase plotted against time for topographic and free waves. The topography was an isolated ridge with $h/d = 0{\cdot}195$; $d/(b-a) = 1{\cdot}71$, $\Omega = 1{\cdot}90$ rad s^{-1}, the wall-to-wall temperature difference was 6·3 K, $B \approx 0{\cdot}04$. ● ● ●, $m = 1$; ○ ○ ○, $m = 2$; — —, $m = 3$. The free wave was $m = 3$; $m = 1$ and $m = 2$ were quasi-stationary. Notice the more complicated relationship of amplitude and phase compared to figure 11.

At lower values of B this simple relationship was replaced by more complicated interactions involving more than two wave components with energy passing round rather that just back and forth, see figure 12.

The time scale of these interactions, 140 s (figure 11) and 180 s (figure 12), is somewhat longer than the spin-up time, $d/(2\,\Omega\nu)^{\frac{1}{2}}$, of about 50 s.

4. Conclusions

The experiments with bottom topography in the absence of free baroclinic waves show that a steady disturbance is forced which is confined to the lower part of the fluid, in contrast to the results of studies of stratified Taylor columns where the topographic disturbance decays more steadily with height. The topographic disturbance has most of its energy in the forced wavenumber and its harmonics. In flows that contain spontaneous baroclinic waves the topographic wave is not trapped but fills the whole fluid. The free waves and topographic waves exchange energy nonlinearly as the free waves drift past the topography.

The work described in this paper was conducted while the author was the recipient of a Natural Environment Research Council Research Studentship. He would also like to thank Dr R. Hide and other members, past and present, of the Geophysical Fluid Dynamics Laboratory for their guidance and support.

REFERENCES

CHARNEY, J. D. & STRAUS, D. M. 1980 Form-drag instability, multiple equilibria and propagating planetary waves in baroclinic, orographically forced, planetary wave systems. *J. Atmos. Sci.* **37**, 1157–1176.

DAVIES, P. A. 1972 Experiments on Taylor columns in rotating stratified fluids. *J. Fluid Mech.* **54**, 691–717.

DOUGLAS, H. A., HIDE, R. & MASON, P. J. 1972 Structure of baroclinic waves. *Quart. J. Roy. Met. Soc.* **98**, 247–263.

EADY, E. T. 1949 Long waves and cyclone waves. *Tellus* **1**, 33–52.

FULTZ, D. & SPENCE, T. 1967 Preliminary experiments on baroclinic westerly flow over a north–south ridge. *Proc. Symp. on Mountain Met., Atmos. Sci. Paper* no. 122, Colorado State University.

HIDE, R. 1961 Origin of Jupiter's Great Red Spot. *Nature* **190**, 895–896.

HIDE, R. & IBBETSON, A. 1966 An experimental study of Taylor columns. *Icarus* **5**, 279–290.

HIDE, R. & MASON, P. J. 1975 Sloping convection in a rotating fluid. *Adv. Phys.* **24**, 47–100.

HIDE, R., MASON, P. J. & PLUMB, R. A. 1977 Thermal convection in a rotating fluid subject to a horizontal temperature gradient: spatial and temporal characteristics of fully developed waves. *J. Atmos. Sci.* **34**, 930–950.

HOGG, N. G. 1973 On the stratified Taylor column. *J. Fluid Mech.* **58**, 517–537.

HOGG, N. G. 1976 On spatially growing baroclinic waves in the ocean. *J. Fluid Mech.* **78**, 217–235.

HUPPERT, H. E. 1975 Some remarks on the initiation of inertial Taylor columns. *J. Fluid Mech.* **67**, 397–412.

INGERSOLL, A. P. 1969 Inertial Taylor columns and Jupiter's Great Red Spot. *J. Atmos. Sci.* **26**, 744–752.

KESTER, J. E. 1966 Thermal convection in a rotating annulus of liquid: nature of the transition from an unobstructed annulus to one with a total radial wall. B.S. thesis, Massachusetts Institute of Technology.

LEACH, H. 1975 Thermal convection in a rotating fluid: effects due to irregular boundaries. Ph.D. thesis, University of Leeds.

REDEKOPP, L. G. 1975 Wave patterns generated by disturbances travelling horizontally in rotating fluids. *Geophys. Fluid Dynamics* **6**, 289–313.

ROBINSON, A. R. 1960 On two-dimensional inertial flow in a rotating stratified fluid. *J. Fluid Mech.* **9**, 321–332.

SZOEKE, R. A. DE 1972 Baroclinic flow over an obstacle in a rotating system. *Woods Hole Ocean. Inst. GFD Notes* **2**, 1–10.

YEH, T.-C. & CHANG, C.-C. 1974 A preliminary experimental simulation of the heating effect of the Tibetan plateau on the general circulation over eastern Asia in summer. *Scienta Sinica* **17**, 397–420.